Journal for ImmunoTherapy of Cancer

Targeting MARCO in combination with anti-CTLA-4 leads to enhanced melanoma regression and immune cell infiltration via macrophage reprogramming

Hidenori Takahashi [1], Patricio Perez-Villarroel [1], Rana Falahat [1], James J Mulé [1,2]

To cite: Takahashi H, Perez-Villarroel P, Falahat R, *et al*. Targeting MARCO in combination with anti-CTLA-4 leads to enhanced melanoma regression and immune cell infiltration via macrophage reprogramming. *Journal for ImmunoTherapy of Cancer* 2025;**13**:e011030. doi:10.1136/jitc-2024-011030

► Additional supplemental material is published online only. To view, please visit the journal online (https://doi.org/10.1136/jitc-2024-011030).

Accepted 03 March 2025

[1]Immunology, Moffitt Cancer Center, Tampa, Florida, USA
[2]Cutaneous Oncology Program, Moffitt Cancer Center, Tampa, Florida, USA

Correspondence to
Dr James J Mulé;
james.mule@moffitt.org

ABSTRACT

Background Strategies to improve the therapeutic efficacy of cancer immunotherapy with immune checkpoint inhibitors include targeting additional immunosuppressive compartments in the tumor microenvironment (TME). Inhibitory macrophages (Mϕ) can be one of the most abundant immune cells in the TME associated with poor prognosis. However, to date, selective Mϕ depletion strategies as a cancer immunotherapy have not been successful in clinical trials. Macrophage Receptor with Collagenous Structure (MARCO) is one of a family of class-A scavenger receptors expressed by Mϕ in the TME and is one of the most upregulated transcripts in dendritic cells (DC) following their ex vivo uptake of dead tumor cells. The clinical significance of MARCO expression in the TME is not fully understood.

Methods The therapeutic potential of targeting MARCO by an anti-murine MARCO (ED31, clone ED31) monoclonal antibody, which inhibits ligand-binding to MARCO, was explored in combination with anti-cytotoxic T-lymphocyte associated protein 4 (anti-CTLA-4) or anti-programmed cell death protein-1 (anti-PD-1) in C57BL/6J mice bearing B16F10 or Pan02 tumors. The mechanism by which ED31 impacts the TME was investigated by flow cytometry in the different treatment arms. The contribution of Mϕ was assessed by both in vivo depletion and in vitro functional assays. Chemokine production was measured by a bead-based multiplex assay.

Results ED31 enhanced antitumor efficacy of anti-CTLA-4, but not of anti-PD-1. Analysis of the TME revealed that adding ED31 to anti-CTLA-4 substantially increased immune cell infiltration, including mature conventional DC recruitment, that was due to a switch to M1-pattern chemokines by Mϕ. Mϕ depletion completely abrogated both the increase in immune cell infiltration and chemokine production, and abolished the antitumor efficacy of the combination therapy.

Conclusions Targeting MARCO as an additional checkpoint in the TME can offer a strategy to improve the antitumor efficacy of anti-CTLA-4 through a mechanism involving Mϕ reprogramming rather than their depletion.

INTRODUCTION

Immune checkpoint inhibitors (ICIs) represented by anti-cytotoxic T-lymphocyte associated protein 4 (anti-CTLA-4) and anti-programmed cell death protein-1 (anti-PD-1)/programmed death-ligand 1 (anti-PD-L1) have demonstrated significant clinical impact in patients with various cancers. Ipilimumab, the first Food and Drug Administration approved anti-CTLA-4 ICI, paved the way to improve overall survival in patients with melanoma as a monotherapy and in combination with anti-PD-1.[1 2] Notwithstanding, there is certainly room for improvement with ICI-based immunotherapies.[3 4] Therefore, elucidating the mechanism that limits the therapeutic efficacy of current ICIs is a cornerstone to improving patient outcomes.

To overcome resistance to ICIs, it is becoming critical to target immunosuppressive compartments in the tumor microenvironment (TME).[5] Macrophages (Mϕ) are one of the most abundant immune cells in the TME, and their presence is related to poor prognosis in several cancer types.[6–8] Various studies have revealed that Mϕ in the TME can promote tumor growth, metastasis, and angiogenesis, as well as suppress antitumor immunity.[6 9 10] Therefore, it is reasonable that targeting Mϕ as a protumoral cell by their depletion or inhibition has been the main strategy to restore antitumor immunity over a decade. However, to date, it remains to be investigated why Mϕ depletion strategies have not been successful in clinical trials.[5 7]

Macrophage Receptor with Collagenous Structure (MARCO) is potentially a promising marker to target Mϕ in the TME.[8 11] MARCO was originally discovered as one of the surface receptors on Mϕ in normal spleen and lymph nodes.[12] It is considered to play an important role in the host defense system and homeostasis of the body as one of the scavenger receptors, and can bind to various ligands, including lipoproteins,

WHAT IS ALREADY KNOWN ON THIS TOPIC

⇒ To date, in vivo macrophage (Mϕ) depletion to improve the therapeutic efficacy of current cancer immunotherapies has not been successful in clinical trials. Macrophage Receptor with Collagenous Structure (MARCO) is one of a family of class-A scavenger receptors expressed by Mϕ in tumor microenvironment (TME) and is one of the most upregulated transcripts in dendritic cells (DC) following their ex vivo uptake of dead tumor cells. The clinical significance of MARCO expression in the TME and ligand-binding on MARCO remains to be elucidated.

WHAT THIS STUDY ADDS

⇒ MARCO is considered an additional checkpoint in the TME. Inhibition of ligand-binding on MARCO can offer a strategy to improve the antitumor efficacy of anti-cytotoxic T-lymphocyte associated protein 4 (anti-CTLA-4), not via Mϕ depletion, by inducing M1-pattern chemokine production and immune cell infiltration with mature conventional DC recruitment in the TME. Ligand-binding on MARCO in the TME could represent one of the potential mechanisms to explain the paucity of immune cell infiltration.

HOW THIS STUDY MIGHT AFFECT RESEARCH, PRACTICE OR POLICY

⇒ These preclinical data support the proof-of-concept that inhibition of ligand-binding on MARCO in combination with anti-CTLA-4 could be useful in cases of immune checkpoint blockade therapy failures, especially for cancer patients with so-called immune desert ("cold") tumors. Adoptive cell therapies such as those that employ chimeric antigen receptor (CAR) - T cell or tumor-infiltrating lymphocyte (TIL) might also be improved in combination with this approach to further promote the infiltration of these systemically administered cells into the TME. This strategy might also have particular promise in neoadjuvant/adjuvant settings for high-risk patients to reduce the recurrence risk by harnessing the conventional DC-T cell priming phase without the use of specific tumor antigens.

bacteria, and dead cells.[8 11–14] Mϕ in the TME have high expression of MARCO, and its expression has association with poor survival in various solid tumors.[15–22] The Cancer Genome Atlas (TCGA) data analysis shows that the expression of MARCO in the TME is significantly increased in many human solid tumors compared with normal tissues.[22]

In addition to MARCO expression on Mϕ in the TME, we have shown previously its expression on dendritic cells (DC) following their loading with tumor lysates, and the importance of targeting MARCO to enhance the efficacy of DC-based tumor vaccines.[23–25] Therefore, MARCO could reasonably be considered a novel target on both Mϕ and DC in the TME to potentially improve the antitumor efficacy of a variety of immune-based therapies. The aim of the current study was to investigate whether targeting MARCO is useful to improve tumor treatments with current immune checkpoint antibodies not through depletion of Mϕ, but rather by both reprogramming Mϕ and using their and DC functions in the TME.

METHODS

Animals

All animal experiments were conducted under an Institutional Animal Care and Use Committee protocol (IS00009850) approved by the Integrity and Compliance board at the University of South Florida and Moffitt Cancer Center in accordance with the US Public Health Service policy and National Research Council guidelines. Wild type C57BL/6J mice and Batf3-knockout (B6.129S(C)-Batf3^{tm1Kmm}/J) mice were obtained from The Jackson Laboratory (Farmington, Connecticut, USA). All experiments were conducted using female mice between the ages of 8 and 10 weeks. Animals were housed in the Comparative Medicine Facilities at the Moffitt Cancer Center. At experimental endpoints, mice were humanely euthanized in accordance with American Veterinary Medical Association guidelines.

Antibodies for treatments

Monoclonal antibody (mAb) of anti-murine MARCO (ED31, clone ED31), which inhibits ligand-binding on MARCO,[12 13] was produced by Leinco Technologies (St. Louis, Missouri, USA). Anti-murine CTLA-4 mAb (anti-CTLA-4, clone 9D9), anti-murine PD-1 mAb (anti-PD-1, clone RMP1-14), isotype mAbs for anti-CTLA-4 (clone MPC-11) and anti-PD-1 (clone 2A3) were purchased from Bio X Cell (West Lebanon, New Hampshire, USA).

Tumor cells

The murine melanoma cell line B16F10 was purchased from ATCC (American Type Culture Collection, Manassas, Virginia, USA); B16-OVA and Pan02 were kindly provided by Dr Pilon-Thomas (Moffitt Cancer Center). Tumor cell lines were cultured in complete Dulbecco's Modified Eagle's Medium (DMEM), except for Pan02, which were cultured in complete Roswell Park Memorial Institute (RPMI) medium.

Murine experiments

Female C57BL/6J mice and Batf3-knockout mice were injected subcutaneously with 1×10^6 B16F10, B16-Ova cells, or 1×10^5 Pan02 in the back. Mice with visible tumors were randomized into treatment arms and treated with a combination of ED31 and anti-CTLA-4 or anti-PD-1, monotherapies, isotype mAbs or phosphate-buffered saline for controls. Tumor growth and survival were measured until the endpoint. Tumor volume measured by an experimenter unblinded to treatment conditions was determined using the formula: $(\text{small diameter})^2 \times (\text{large diameter}) \times 0.5$.

Immune cell depletions

To deplete effector cells in vivo, mice were injected intraperitoneally with anti-CD8 (clone 2.43, Bio X Cell), anti-CD4 (clone GK1.5, Bio X Cell), or anti-NK1.1 (clone PK136, Bio X Cell) antibodies 1 day before the initiation of treatment and continued twice weekly. For Mϕ depletion, anti-CSF1R antibody (clone AFS98, Bio X Cell) or isotype antibody (Bio X Cell) were started 1 day before

the initiation of treatment and continued every other day. Cellular depletions were confirmed by flow cytometry.

TME analysis

Single-cell suspensions from harvested tumors prepared by using the Mouse Tumor Dissociation Kit (Miltenyi) according to the manufacturer's protocol were stained with a combination of fluorescently conjugated anti-mouse mAbs for cell surface phenotyping (online supplemental methods). For intracellular staining, cells were permeabilized and fixed using the eBioscience Intracellular Fixation and Permeabilization Buffer set (Invitrogen) following the manufacturer's protocol. For interferon (IFN)-γ staining, cells were incubated for 4 hours at 37°C with Leukocyte Activation Cocktail (BD Bioscience), and intracellular staining was done by using the BD Cytofix/Cytoperm Fixation/Permeabilization Kit (BD Biosciences). Cell phenotypes were measured on BD LSR II cytometer (BD Biosciences) and analyzed by using FlowJo software (BD Biosciences).

For immunohistochemical staining, formalin-fixed tumor tissues were stained using anti-CD45 antibody (Abcam) with red chromogen using a Ventana Discovery XT automated system (Ventana Medical Systems, Tucson, Arizona, USA) as per manufacturer's protocol.

In vivo chemokine analysis using harvested tumor

Single-cell suspensions from harvested tumors using the Mouse Tumor Dissociation Kit (Miltenyi) were cultured for 24 hours. Chemokine concentrations of supernatants were analyzed using a Multiplex Assay Kit (LEGENDplex, BioLegend).

In vitro chemokine analysis using murine bone marrow-derived Mφ and DC

For bone marrow-derived Mϕ (BM-Mϕ) cultures, murine bone marrow cells were re-suspended in comple DMEM with recombinant mouse macrophage colony-stimulating factor (M-CSF, PeproTech). After a 7-day culture with M-CSF, adherent cells were gently detached using a cell scraper and polarized to induce various Mϕ phenotypes; M1-Mϕ produced by stimulation with IFN-γ and lipopolysaccharide, M2-Mϕ with interleukin (IL)-4, and TAM (tumor-associated macrophage)-like Mϕ with supernatants collected from B16F10 tumor cell line culture.

For bone-marrow-derived DC (BM-DC) cultures, the bone marrow cells were re-suspended in complete RPMI medium with recombinant mouse granulocyte/GM-CSF (PeproTech) and IL-4. After 7-day culture, non-adherent cells were collected. To produce tumor lysate pulsed DC (TL-DC), collected cells (Un-DC) were pulsed with B16F10-derived tumor lysates at a ratio of 1 DC to 3 cells lysate equivalents for 24 hours. B16F10-derived tumor lysate was prepared as described previously.[23–25]

Single-cell suspensions of BM-Mϕ or BM-DC were cultured for 24 hours with or without ED31 exposure (20 µg/mL) simultaneously during the polarization process. Chemokine concentrations of supernatants were analyzed using the Multiplex Assay Kit (LEGENDplex, BioLegend).

Statistics

Prism V.10 software (GraphPad Software) was used to create graphs and conduct statistical analyses. Specific statistical tests are indicated in each figure legend. For survival analysis, Kaplan-Meier's method and log-rank (Mantel-Cox) test were performed to compare differences among curves. A formal power calculation was not performed. In vivo and in vitro data are representative of at least two repeats unless stated otherwise. All error bars indicate mean±SEM values of $p<0.05$ were considered significant.

RESULTS

Targeting MARCO by ED31 enhances antitumor efficacy of anti-CTLA-4, but not of anti-PD-1

We first explored the therapeutic potential of targeting MARCO by using ED31 in combination with anti-CTLA-4 or anti-PD-1. After implantation of B16F10 melanoma, treatment of anti-CTLA-4 was simultaneously administered in combination with or without ED31 three times in different treatment timelines: initiated early on day 3 (figure 1A–C), initiated on day 7 for established tumors (>30 mm^3, figure 1D–F), or initiated on day 14 for large tumors (>100 mm^3, figure 1G–I). The addition of ED31 to anti-CTLA-4 consistently enhanced antitumor efficacy both in tumor growth and in survival regardless of the timing of treatment. ED31 monotherapy did not result in an antitumor effect in this model, including early on at day 3 after tumor cell injection. The addition of ED31 could enhance the antitumor efficacy of anti-CTLA-4 against large tumors in which anti-CTLA-4 monotherapy had no impact (figure 1H,I). We also explored the combination therapeutic efficacy in another tumor line, namely the murine pancreas carcinoma Pan02, which again showed a superior antitumor effect in both tumor growth and survival (online supplemental figure 1).

We next investigated the combination of ED31 with anti-PD-1 in the same B16F10 melanoma model. In this case, adding ED31 to anti-PD-1 failed to show a superior antitumor effect compared with anti-PD-1 monotherapy (figure 1J). Repeated experiments using the same treatment protocol as figure 1D (treatment on day 7, 10, 13) revealed that adding ED31 can enhance antitumor efficacy only when administered together with anti-CTLA-4 (figure 1K), but not with anti-PD-1 (figure 1J).

Taken together, we conclude that targeting MARCO by ED31 can enhance antitumor efficacy only in combination with anti-CTLA-4. Therefore, we next investigated the mechanism operative in vivo by this specific therapeutic combination.

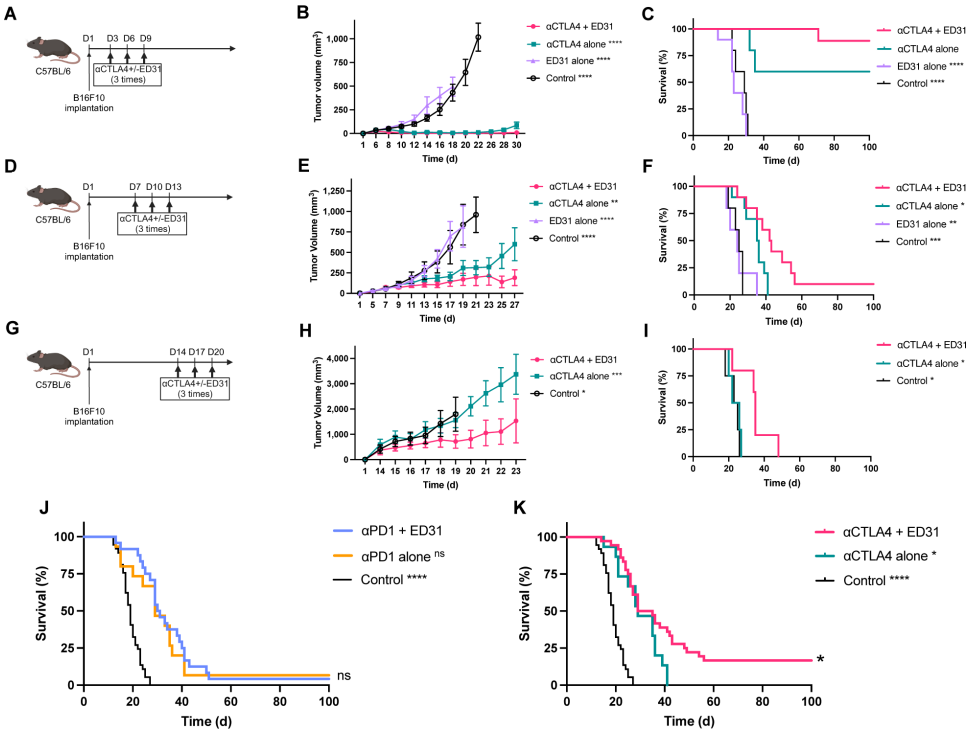

Figure 1 Adding ED31 to anti-CTLA-4 (αCTLA-4), but not to anti-PD-1 (αPD-1) can enhance antitumor efficacy in vivo. (A–I) C57BL/6J mice injected with B16F10 melanoma were treated at different timelines as indicated. (A–C) Treatment initiated early on day 3. n=9 (αCTLA-4+ED31), n=5 (αCTLA-4 alone), n=10 (ED31 alone), n=5 (Control). (D–F) Treatment initiated on day 7 for established tumors (>30 mm^3). n=10 (αCTLA-4+ED31), n=10 (αCTLA-4 alone), n=5 (ED31 alone), n=5 (Control). (G–I) Treatment initiated on day 14 for large tumors (>100 mm^3). n=5 (αCTLA-4+ED31), n=4 (αCTLA-4 alone), n=4 (Control). These results were from one experiment, representative of at least two independent experiments. For tumor growth curves (B,E,H), *p<0.05; **p<0.01; ***p<0.001; ****p<0.0001; versus αCTLA-4+ED31 by two-way analysis of variance test. For survival curves (C,F,J), *p<0.05; **p<0.01; ***p<0.001; ****p<0.0001; versus αCTLA-4+ED31 by log-rank (Mantel-Cox) test. (J–K) C57BL/6J mice with B16F10 were treated with αPD-1+ED31 (J) or αCTLA-4+ED31 (K), or monotherapies as indicated in (D). These results were compiled from three independent consecutive experiments. (J) Survival comparison between αPD-1+ED31 (n=25) or αPD-1 alone (n=15). No statistical difference (ns) by log-rank (Mantel-Cox) test. HR (Mantel-Haenszel)=0.86 (95% CI; 0.42 to 1.76). (K) Survival comparison between αCTLA-4+ED31 (n=35) or αCTLA-4 alone (n=15). *p<0.05 versus αCTLA-4+ED31 by log-rank (Mantel-Cox) test. HR (Mantel-Haenszel)=0.45, (95% CI; 0.21 to 0.96). CTLA-4, cytotoxic T-lymphocyte associated protein 4; PD-1, programmed cell death protein-1.

Adding ED31 to anti-CTLA-4 significantly increases immune cell infiltration in the TME

To elucidate the mechanism by which ED31 enhances antitumor efficacy of anti-CTLA-4 when employed in combination, we explored the immune cell infiltrate profile in the TME. Tumor samples were collected 3 days after a single drug administration and analyzed to compare the immune cell profile among the four different treatment arms (combination with anti-CTLA-4 and ED31 vs anti-CTLA-4 monotherapy vs ED31 monotherapy vs control) by flow cytometry and immunohistochemistry (figure 2A). We first found a significant increase in the total immune cell density (the total cell number of $CD45^+$ cells per tumor area in the TME) in the combination treatment arm (figure 2B). This increase was observed only in the combination therapy and not in the monotherapy arms and was confirmed by immunohistochemistry analysis (figure 2C). Regarding subpopulation analysis among $CD45^+$ immune cells in the TME, a broad group of lymphocytes and myeloid cells, not a specific group of cells, was significantly increased in the combination arm of ED31 and anti-CTLA-4 (figure 2D,E). A single administration of this combination therapy induced a rapid increase in the number of a variety of lymphocytes in the TME, including $CD8^+$ T cells, $CD4^+$ T cells, natural killer (NK) cells, and B cells (figure 2D). In addition, an increase in myeloid cell populations was also detected only in the combination arm of ED31 and anti-CTLA-4, including Mϕ and conventional DC (cDC). Moreover, a significant increase of M1-like Mϕ ($CD86^+$Mϕ) and mature cDC ($CD86^+$ cDC) were observed only in the combination arm (figure 2E).

As was shown by the survival curve in figure 1J, the combination therapy with ED31 and anti-CTLA-4 resulted in the so-called "typical" delayed separation curve with long-tail effect, which was not observed in the combination of ED31 with anti-PD-1 (figure 1K). This feature has been observed in randomized clinical trials of ICIs, which can implicate the operative existence of DC-based cancer immunity.[3–5] It is well established that mature cDC is the most potent antigen-presenting cell that can activate a tumor-specific T-cell response.[26] We have already found that the combination therapy can increase mature

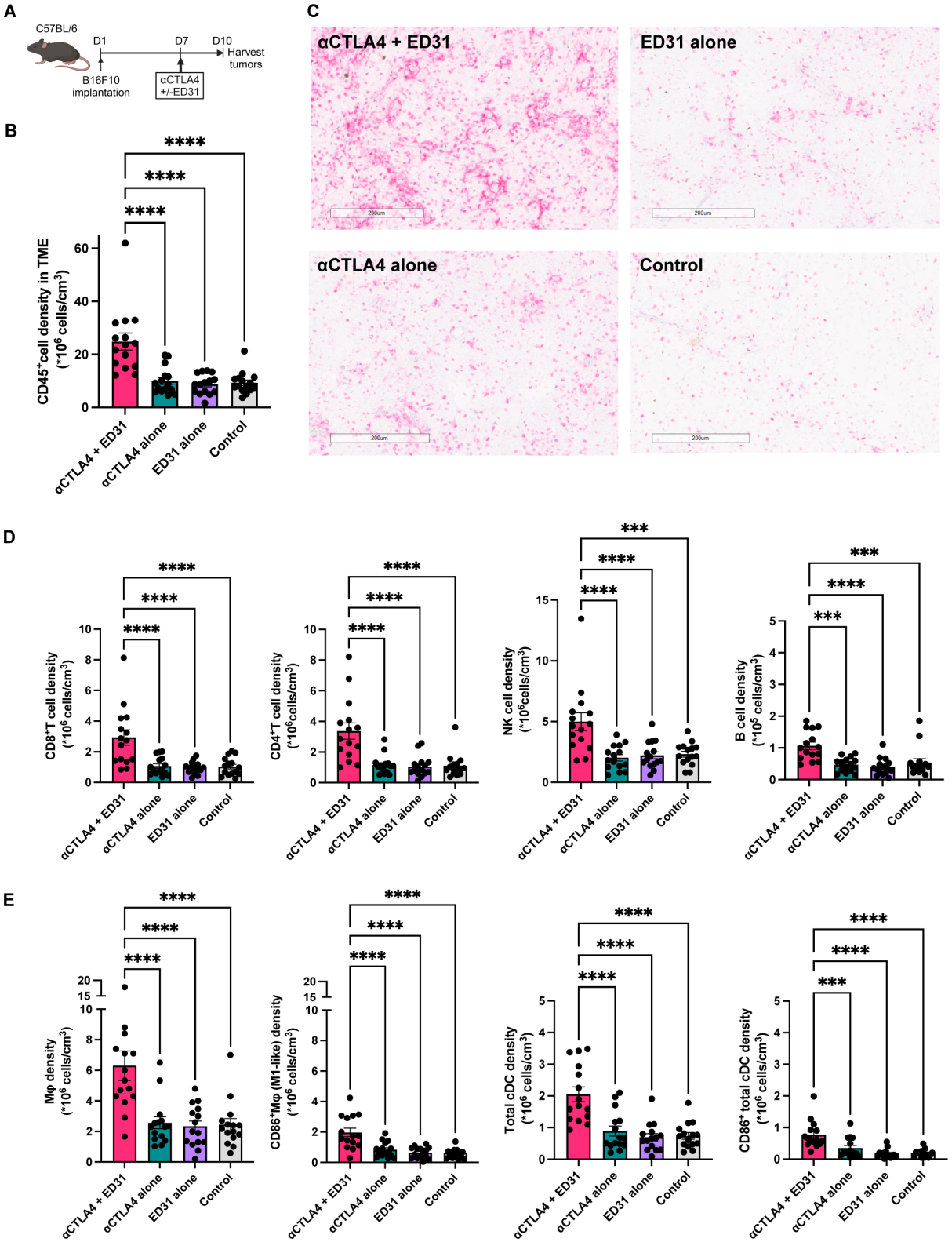

Figure 2 Adding ED31 to anti-CTLA-4 can significantly increase immune cell infiltration in the TME. (A) Timeline of the experiment. (B) Total immune cells ($CD45^+$) density (10^6 cells/cm^3) in the TME on day 10. (C) Representative immunohistochemistry images of tumor samples. $CD45^+$ cells were stained with red chromogen. Scale bar, 200 µm. (D) Cell density (10^6 cells/cm^3) among subpopulations of lymphoid cells ($CD45^+CD11b^-$) in the TME. (E) Cell density (10^6 cells/cm^3) among myeloid cells in the TME. Mϕ was defined as $CD45^+CD11b^+F4/80^+$, and total cDC as the sum of cDC_1 ($CD45^+CD11b^-CD11c^+$) and cDC_2 ($CD45^+CD11b^+CD11c^+$). $CD86^+$Mϕ and $CD86^+$DC were considered as M1-like Mϕ and mature cDC, respectively. These results were compiled from three independent consecutive experiments. n=15 per group. ***p<0.001; ****p<0.0001; versus αCTLA-4+ED31 by one-way analysis of variance test. cDC, conventional dendritic cell; CTLA-4, cytotoxic T-lymphocyte associated protein 4; Mϕ, macrophages; NK, natural killer; TME, tumor microenvironment.

cDC in the TME (figure 2E). In addition, we noticed that the long-term surviving mice developed vitiligo (online supplemental figure 2A), which is known to have clinical association with favorable responses to immunotherapy in patients with melanoma.[27 28] Indeed, a preliminary experiment shows that four of five long-term selected survivors successfully rejected a re-challenge of viable B16F10 melanoma cells for at least 6 months after the combination therapy with ED31 and anti-CTLA-4. Therefore, we next hypothesized that adding ED31 to anti-CTLA-4 can induce superior tumor-antigen specific cytotoxic T cell (CTL) immunity. Using an Ova-expressing B16 melanoma bearing mouse model, we determined if a change existed in tumor-antigen specific CTL in the TME. Indeed, adding ED31 to anti-CTLA-4 induced superior tumor growth inhibition with significantly higher immune cell infiltration with functional Ova-specific CTL in the TME (online supplemental figure 2B–E). This result is coincident with the increase of mature cDC in TME induced by adding ED31 to anti-CTLA-4 (figure 2E).

Thus, ED31 added to anti-CTLA-4 can significantly increase immune cell infiltration in the TME that include a variety of effector T cells, M1-like Mϕ, and mature cDC. Neither anti-CTLA-4 nor ED31 as a monotherapy can increase the immune cell density in the TME.

Adding ED31 to anti-CTLA-4 increases M1-pattern chemokines via Mϕ in the TME

Given that adding ED31 to anti-CTLA-4 can increase a variety of immune cell types in the TME through its action on Mϕ, we next studied the mechanism by which Mϕ may promote it. The increase of immune cell infiltration in the TME led our attention to a chemokine analysis because of their known ability to guide the migration of various immune cells.[29 30] To examine whether ED31 can directly act on Mϕ to increase chemokine production, we first conducted in vitro experiments using mouse BM-Mϕ. BM-Mϕs produced in vitro were then polarized to four different phenotypes, that is, M0-Mϕ (without activation), M1-Mϕ (polarized with IFN-γ and lipopolysaccharide), M2-Mϕ (polarized with IL-4), and TAM-like Mϕ (polarized with centrifuged supernatants collected from B16F10 cell line culture medium). We then analyzed chemokine concentrations in the supernatants by multiplex ELISA assay to determine whether in vitro ED31 exposure affected chemokine production by these polarized BM-Mϕs (figure 3A). Without ED31 exposure, only M1-Mϕ showed strong chemokine production. After in vitro ED31 exposure for 24 hours, while M1-Mϕ did not change chemokine levels, such exposure significantly induced the production of various chemokines by M0-Mϕ, M2-Mϕ, and TAM-like Mϕ (figure 3A). Moreover, it is noteworthy that the cluster of induced chemokines in each BM-Mϕ was almost identical to the cluster of chemokines observed in M1-Mϕ, that is, CXCL1, CXCL10, CCL2, CCL3, CCL4, CCL5, and CCL22 (figure 3A). We also confirmed that in vitro ED31 exposure on TAM-like Mϕ can enhance the M1-pattern of chemokine production in a dose-dependent manner (online supplemental figure 3). On the other hand, anti-CTLA-4 exposure to BM-Mϕ did not affect chemokine production by all the Mϕ subsets studied (online supplemental figure 4). In addition, expression of various Mϕ surface markers did not show any significant changes after ED31 exposure, regardless of combination with or without anti-CTLA-4 (online supplemental figure 5). Therefore, these results indicate that ED31 can directly act to reprogram Mϕ to induce the production of M1-pattern chemokines without notable surface marker changes.

We also examined whether ED31 can directly act on DC to increase chemokine production by using two phenotypes of mouse BM-DC, including TL-DC (pulsed with B16F10 tumor lysate) and Un-DC (without B16F10 tumor lysate pulse). Without ED31 exposure, both BM-DCs showed distinct chemokine production, especially in CCL17 and CCL22 (figure 3B). However, contrary to the striking ED31 effect on BM-Mϕs, both BM-DCs did not increase chemokine production, except for some small changes (figure 3B). This observation argues that it is unlikely that ED31 acts mainly on DC to increase chemokine production in the TME. We also investigated in vitro ED31 impact on chemokine production on other cell types or whole tissue samples and confirmed that ED31 exposure did not change chemokine production by the B16F10 melanoma cell line, or by spleen and lymph node preparations, except for whole tumor tissue samples (online supplemental figure 6).

We next conducted in vivo experiments to further confirm that adding ED31 to anti-CTLA-4 increases chemokine production in the TME via Mϕ. First, we collected tumor samples after in vivo administration of the treatments and then analyzed chemokine concentrations in the TME between the four different arms (combination with anti-CTLA-4 and ED31 vs anti-CTLA-4 monotherapy vs ED31 monotherapy vs control). As expected, adding ED31 to anti-CTLA-4 significantly increased various chemokine levels in the TME among M1-pattern chemokines, especially CXCL10, CCL4, CCL5, and CCL22 (figure 3C, online supplemental figure 7).

To confirm that the increased chemokines in the TME are derived from Mϕ, we next conducted in vivo Mϕ depletion studies. We evaluated the effect of Mϕ depletion on chemokine levels in the TME after single combination therapy with or without the addition of anti-CSF1R. As expected, we verified that Mϕ depletion during the combination therapy significantly abrogated the increase in the chemokines, which are almost identical to the M1-pattern of chemokines, namely CXCL1, CXCL10, CCL2, CCL3, CCL4, CCL5, and CCL22 (figure 3D, online supplemental figure 8).

Taken together, these in vitro and in vivo results demonstrate that adding ED31 to anti-CTLA-4 can increase M1-pattern chemokines in the TME produced by Mϕ.

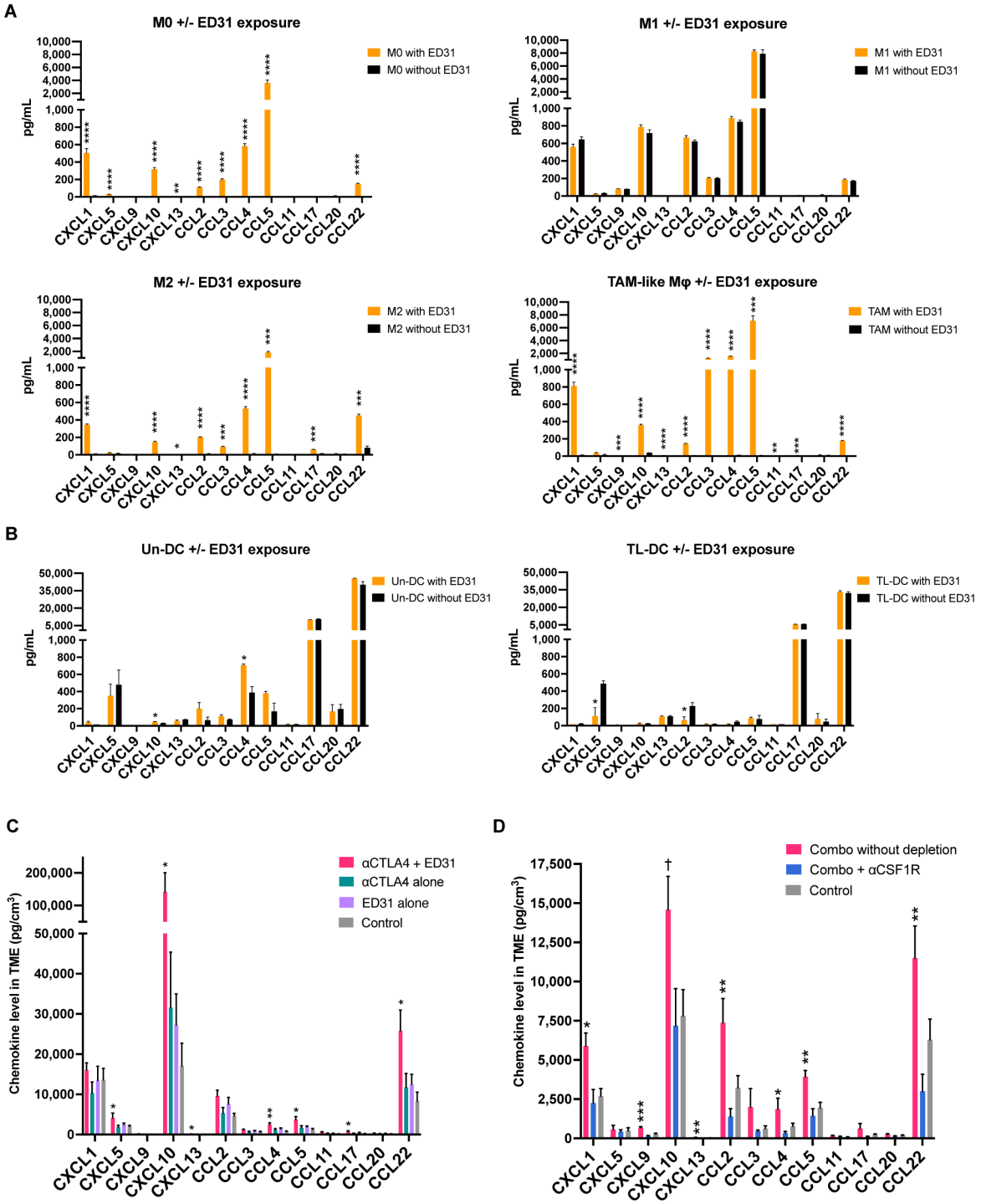

Figure 3 ED31 can induce M1-pattern chemokine production from ex vivo BM-Mϕ and in vivo Mϕ in the TME. (A) Chemokine concentrations in supernatants collected from four different classical phenotypes of ex vivo BM-Mϕ (indicated as M0, M1, M2, TAM-like Mϕ) after 24 hours culture with or without in vitro ED31 exposure. n=3 per group. **p<0.01; ***p<0.001; ****p<0.0001; by unpaired t-test. (B) Chemokine concentrations in supernatants collected from ex vivo bone-marrow derived DC (indicated as Un-DC, TL-DC) after 24-hour culture with or without in vitro ED31 exposure. n=3 per group. *p<0.05; by unpaired t-test. (C) Chemokine level (pg/cm^3) in the TME 1 day after the treatment as indicated. n=5 (αCTLA-4+ED31), n=6 (αCTLA-4 alone), n=6 (ED31 alone), n=6 (Control). *p<0.05; **p<0.01; versus αCTLA-4+ED31 by one-way ANOVA test (individual values of chemokines are shown in online supplemental figure 7). (D) Chemokine level (pg/cm^3) in the TME after single combination therapy with αCTLA-4 and ED31 (Combo) with or without anti-CSF1R (αCSF1R). n=4 (Combo without depletion), n=4 (Combo+αCSF1R), n=5 (Control). †p=0.057; *p<0.05; **p<0.01; ***p<0.001; versus Combo without depletion by one-way ANOVA test (individual values of chemokines are shown in online supplemental figure 8). The results were from one experiment, representative of two independent experiments. ANOVA, analysis of variance; BM-Mϕ, bone marrow derived macrophage; CTLA-4, cytotoxic T-lymphocyte associated protein 4; DC, dendritic cell; TAM, tumor-associated macrophage; TL-DC, tumor lysate pulsed DC; TME, tumor microenvironment; UN-DC, collected cells DC.

Mϕ depletion completely abrogates the increase of immune cell infiltration in the TME and antitumor efficacy of the combination therapy

To confirm that the increase of immune cell infiltration in the TME induced by adding ED31 to anti-CTLA-4 contributes to the therapeutic effect, we first conducted in vivo depletion experiments against effector immune cells, that is, $CD8^+$ T cell, $CD4^+$ T cell, and NK cells, respectively (figure 4A,B). As expected, CD8 depletion strongly canceled the antitumor effect both in tumor growth curves and in animal survival. In addition, CD4 depletion or NK depletion significantly decreased the antitumor effect of the combination therapy, respectively. Thus, these results demonstrate that each effector cell type has its own role in the therapeutic effect of this combination therapy and strengthen the evidence that adding ED31 to anti-CTLA-4 can enhance antitumor efficacy by promoting various immune cell infiltration into the TME.

Therefore, to determine whether the addition of ED31 induces the increase of all effector cell types in the TME through its action on Mϕ, we next conducted in vivo Mϕ depletion. As expected, Mϕ depletion completely abolished the antitumor efficacy as measured by both tumor growth and animal survival (figure 4C,D). Regarding the immune cell profile in the TME, Mϕ depletion likewise completely abrogated the increase of immune cell infiltration of not only effector T and NK cells, but also B cells and cDC populations, including mature cDC infiltration into the TME (figure 4E–H). From the comparison with the control group, the administration of anti-CSF1R, which is commonly used to deplete Mϕ,[27] specifically depleted Mϕ but did not affect cDC populations (figure 4H). In contrast, anti-CSF1R administration abrogated the increase in changes of cDC and T cells that should have been induced by the combination therapy, especially at later time points (figure 4H,I). Therefore, it is the increase of cDC-T cell populations in the TME by the combination therapy that is also induced by the reprogramming of Mϕ function.

Taken together, these depletion studies directly demonstrate the pivotal role of Mϕ in this combination therapy and clarify the mechanism that adding ED31 to anti-CTLA-4 can promote a variety of immune cell infiltrates, including mature cDC, in the TME through the function of reprogrammed Mϕ and production of chemokines.

Combination with anti-CTLA-4, not anti-PD-1, is necessary for ED31 to elicit immune cell infiltration including mature cDC into the TME

We have demonstrated that adding ED31 to anti-CTLA can enhance the antitumor efficacy by inducing broad immune cell infiltration in the TME through an increase of M1-pattern chemokines produced by Mϕ. However, there is a need to elucidate the reasons why ED31 requires anti-CTLA-4, why ED31 monotherapy cannot show antitumor efficacy, and why adding ED31 to anti-PD-1 did not improve antitumor therapeutic efficacy. To elucidate a reason why ED31 requires that it be administered in combination with anti-CTLA-4 but not with anti-PD-1, we compared the immune profile in the TME between the combination of ED31 with anti-CTLA-4 versus with anti-PD-1 (figure 5A). Although both combination therapies increased $CD8^+$ T cells in the TME compared with the control, only the combination with anti-CTLA-4 showed a significant increase in the total number of $CD45^+$ immune cells containing a wide variety of immune cell infiltrates, including $CD4^+$ T cells, NK cells, B cells, and mature cDC in the TME (figure 5B,C). We also confirmed that ED31 with anti-CTLA-4, but not with anti-PD-1, significantly increased M1-pattern chemokines in the TME (figure 5D, online supplemental figure 9).

Of note, the increased proportion of mature cDC (%$CD86^+$ cDC among $CD45^+$ cells) was the only significant distribution change (online supplemental figure 10). Considering that neither ED31 monotherapy nor anti-CTLA monotherapy increased mature cDC in TME (figure 2E), this increase was elicited only by the combination of ED31 with anti-CTLA-4. To confirm the importance of mature cDC recruitment into the TME, we conducted in vivo experiments using cDC_1 knockout mice ($Batf3^{-/-}$ mice, figure 5E). The combination therapy against $Batf3^{-/-}$ mice indeed failed to increase the variety of immune cell infiltrates in the TME (figure 5F–H). Analysis of the subpopulation of cDC confirmed that the increase of cDC_1, but not cDC_2, was abrogated in the $Batf3^{-/-}$ mice (figure 5H). These results revealed that mature cDC_1 was essential for the combination therapy to induce immune cell infiltration in the TME.

In sum, ED31 administered with anti-CTLA-4, but not with anti-PD-1, elicited effective immune cell infiltration with mature cDC_1 recruitment in the TME. The findings further showed the importance of both reprogramming Mϕ and harnessing cDC_1 simultaneously to achieve successful tumor regression.

DISCUSSION

In this study, we demonstrated that targeting MARCO by ED31 can improve the antitumor efficacy of anti-CTLA-4 and uncovered the mechanism of action. Importantly, ED31 could enhance antitumor efficacy by utilization of Mϕ, not by their depletion. ED31 was found to reprogram Mϕ to produce M1-pattern chemokines, leading to heightened immune cell infiltration in the TME and their functional activation through the administration of anti-CTLA-4. From this point of view, MARCO might be considered as an Mϕ immune checkpoint in the TME.

We believe our study has several important considerations in the current ICI era. First, our study demonstrated the significance of using Mϕ rather than eliminating them to induce effective immune cell infiltration into the TME. Second, rather than attempting to deplete Mϕ in the TME, targeting scavenger receptors to reprogram and restore positive functions through switching to M1-pattern chemokine production appears to be a viable

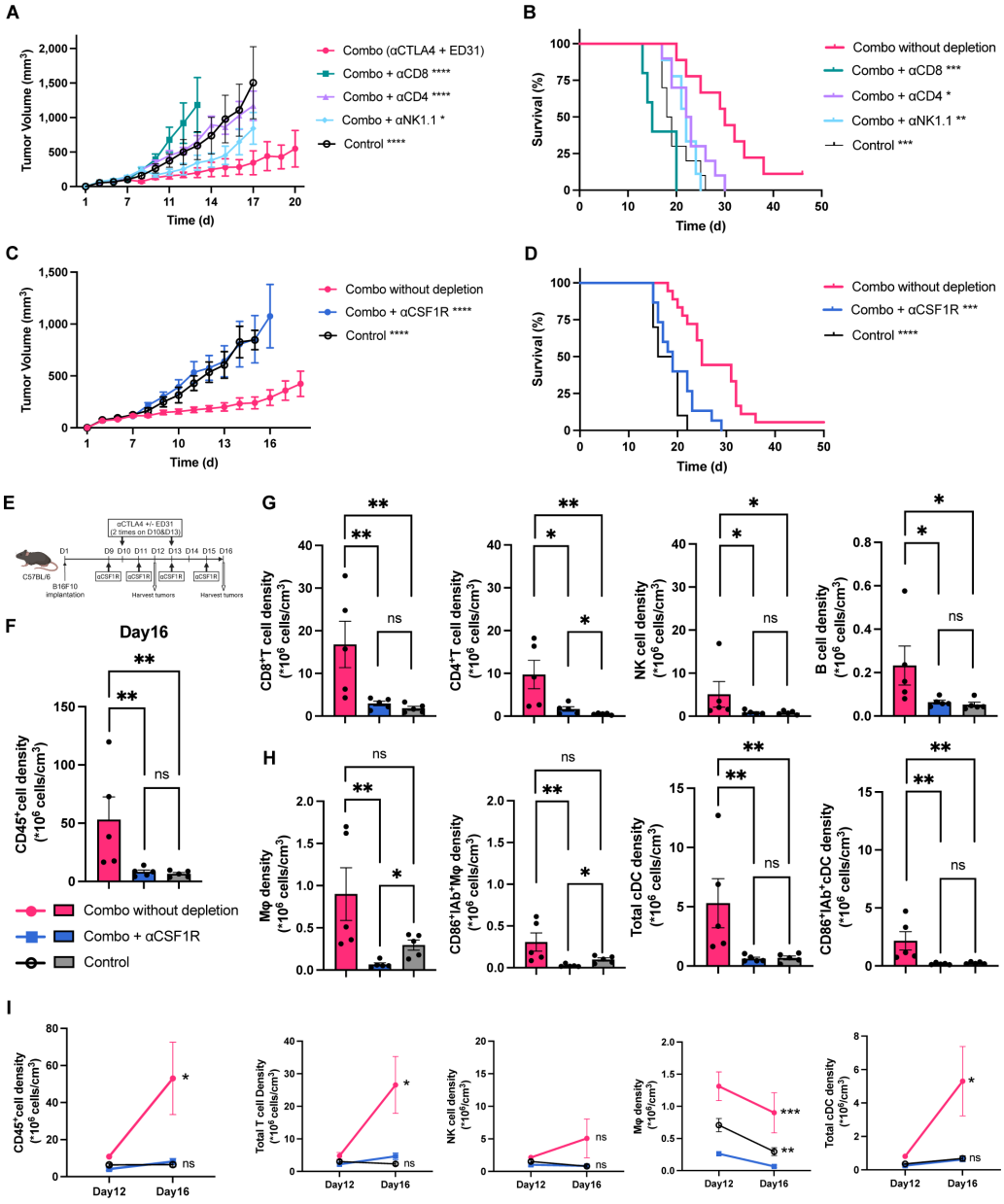

Figure 4 Mϕ depletion completely abrogates the antitumor efficacy of the combination therapy and eliminates the increase in immune cell infiltration in the TME. (A–D) C57BL/6J mice with B16F10 were treated with Combo (αCTLA-4+ED31, three times on day 7, 10, 13) in combination with depletion antibodies specific for the indicated surface markers. (A–B) Depletion experiment against effector cells. (A) Tumor growth curve from one experiment, representative of two independent experiments. n=5 per group. *p<0.05; ****p<0.0001; versus Combo without depletion by two-way ANOVA test. (B) Survival comparison among Combo without depletion (n=9), with αCD8 (n=5), αCD4 (n=10), αNK1.1 (n=9), or Control (n=10). Data were compiled from two independent experiments. *p<0.05; **p<0.01; ***p<0.001; versus Combo without depletion by log-rank (Mantel-Cox) test. (C–D) Depletion experiment against Mϕ using αCSF1R. (C) Tumor growth curve from one experiment, representative of two independent experiments. n=8 (Combo without depletion), n=7 (Combo+αCSF1R), n=5 (Control). ****p<0.0001; versus Combo without depletion by two-way ANOVA test. (D) Survival comparison among Combo without depletion (n=18), Combo+αCSF1R (n=15), or Control (n=10). Data were compiled from two independent experiments. ***p<0.001; ****p<0.0001; versus Combo without depletion by log-rank (Mantel-Cox) test. (E–I) Mϕ depletion experiment for TME analysis. The results were from one experiment, representative of two independent experiments. (E) Timeline of the experiment. Tumors were harvested on day 12 and day 16 after the combination therapy (on day 10, 13) with or without αCSF1R (every other day on day 9, 11, 13, 15). n=10 per group. (F) $CD45^+$ cell density (10^6 cells/cm^3) in the TME. (G) Cell density (10^6 cells/cm^3) among subpopulations of effector cells in the TME. (H) Cell density (10^6 cells/cm^3) among myeloid cells in the TME. Mϕ and total cDC were defined as the same in figure 2E. $CD86^+IAb^+$Mϕ and $CD86^+IAb^+$cDC cells were considered as M1-like Mϕ and mature cDC, respectively. *p<0.05; **p<0.01; by Mann-Whitney test. (I) Changes of cell density in the TME over time. Tumors were harvested on day 12 and 16 using the same cohort. *p<0.05; **p<0.01; ***p<0.001; versus Combo+anti-CSF1R by two-way ANOVA test. ANOVA, analysis of variance; cDC, conventional dendritic cell; CTLA-4, cytotoxic T-lymphocyte associated protein 4; Mϕ, macrophages; NK, natural killer; TME, tumor microenvironment.

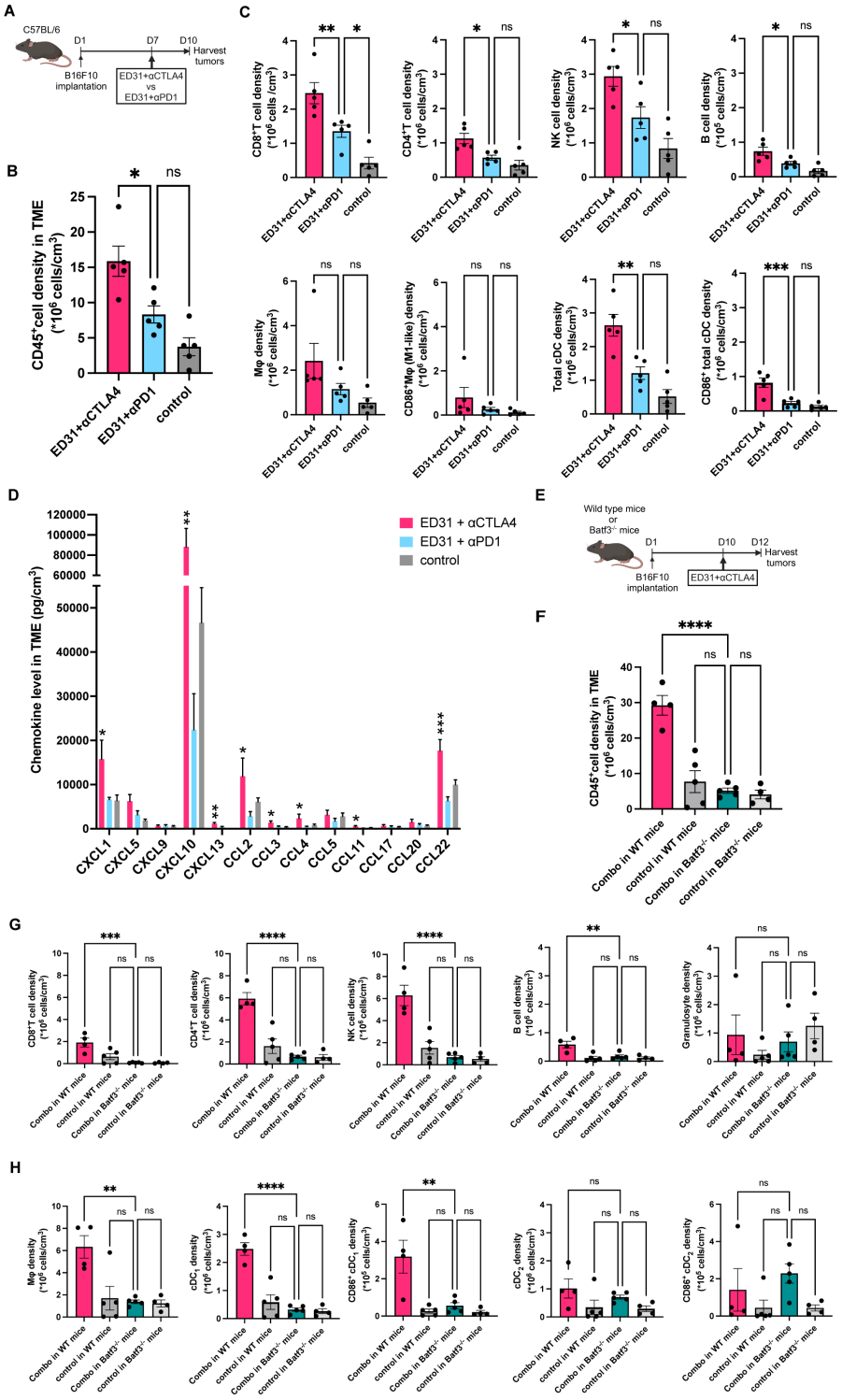

Figure 5 Combination of ED31 with anti-CTLA-4, but not with anti-PD-1, can induce higher effector cell infiltration with mature cDC in the TME. (A) Timeline of the experiment. C57BL/6J mice with B16F10 were treated with the combination therapy of ED31 with αCTLA-4 or with αPD-1 on day 7, and tumors harvested on day 10 were analyzed. (B) $CD45^+$ cell density (10^6 cells/cm^3) in the TME. (C) Cell density of each immune subpopulation (10^6 cells/cm^3) in the TME. *p<0.05; **p<0.01; ***<0.001; by one-way ANOVA test. (D) Chemokine level (pg/cm^3) in the TME after single combination therapy with the combination therapy of ED31 with αCTLA-4 or with αPD-1. n=5 (ED31+αCTLA-4), n=6 (ED31+αPD-1), n=7 (control). *p<0.05; **p<0.01; ***p<0.001; versus ED31+αPD-1 by one-way ANOVA test (individual values of chemokines are shown in online supplemental figure 9). (E) Timeline of the experiment. Wild type (C57BL/6J) mice or $Batf3^{-/-}$ mice with B16F10 were treated with the combination therapy of ED31 with αCTLA-4 on day 10, and tumors harvested on day 12 were analyzed. (F) $CD45^+$ cell density (10^6 cells/cm^3) in the TME. (G–H) Cell density of each immune subpopulation (10^6 cells/cm^3) in the TME. *p<0.05; **p<0.01; ***<0.001; by one-way ANOVA test. ANOVA, analysis of variance; cDC, conventional dendritic cell; CTLA-4, cytotoxic T-lymphocyte associated protein 4; Mϕ, macrophages; NK, natural killer; PD-1, programmed cell death protein-1; TME, tumor microenvironment.

alternative. Third, the utilization of reprogrammed Mϕ is not in and of itself sufficient to cause effective tumor regression.

We demonstrated that targeting MARCO by ED31 can improve the antitumor efficacy of anti-CTLA-4, even against large established tumors refractory to anti-CTLA-4 monotherapy (figure 1G–I). Furthermore, we elucidated the mechanism of therapeutic efficacy of this combination therapy through both immune cell infiltration and activation. It is widely recognized that the therapeutic efficacy of current immunotherapies depends, in part, on the pre-existence of immunity in the TME, and approaches to induce a favorable TME for antitumor immunity with high immune cell infiltration are needed to enhance the potency of immune-based therapies.[5] Most clinical responses to ICIs occur when a tumor exhibits the inflamed "hot" immunotype, but not "cold" immune desert contexture.[31] Therefore, our combination therapy could be a promising approach, especially in this regard. The existence of Mϕ in TME has been historically considered as one of the immuno-suppressive features, and clinical trials to target Mϕ have been focusing on inhibition of Mϕ recruitment into TME or depletion of Mϕ.[5–7 9 10] In contrast, our study revealed that an Mϕ utilization approach through reprogramming could transform the TME into a favorable immune profile with higher immune cell infiltration and revealed the importance of not only focusing on T cell-based immunity, but also harnessing innate immunity including NK cells and Mϕ. Our findings might also contribute to elucidating one of the mechanisms of formation of TME desert immunotypes, and this combination therapy of ED31 and anti-CTLA-4 could be useful especially for such tumors. Moreover, adoptive cell therapies such as chimeric antigen receptor (CAR) - T cell or tumor-infiltrating lymphocyte (TIL) therapy may also be promising in combination with this Mϕ reprogramming and utilization approach to promote infiltration of the administered adoptive cells into the TME.

We uncovered the mechanism by which targeting MARCO could restore the function of Mϕ to produce M1-pattern chemokines CXCL1, CXCL10, CCL2, CCL3, CCL4, CCL5, and CCL22. These M1-pattern chemokines are well known to induce infiltration of various immune cells into the TME.[29 30] Our previous studies revealed the effect of each chemokine on the migration capacity of various effector cells.[32] We also had identified a unique chemokine gene expression signature associated with immune cell infiltration in the TME and better patient outcome, which encodes 12 distinct chemokines (CCL2, CCL3, CCL4, CCL5, CCL8, CCL18, CCL19, CCL21, CXCL9, CXCL10, CXCL11, and CXCL13).[33–35] Other investigators also reported similarly that a subset of six chemokines (CCL2, CCL3, CCL4, CCL5, CXCL9, and CXCL10) are important for the recruitment of activated T cells into the TME.[36] Although chemokines involved in the recruitment of cDC into the TME have been less studied compared with T cells, at least CCL4 and CCL5 have been reported as chemokines crucial for the recruitment of cDC into TME.[37–39] In contrast, one of the increased chemokines, CCL22, is known for its capacity to recruit regulatory T cells.[30] This increase might be one of the reasons why ED31 monotherapy cannot show antitumor efficacy. Altogether, we conclude that the addition of ED31 to anti-CTLA-4 could increase M1-pattern chemokine production by reprogramming and using Mϕ, promoting the infiltration of various immune cells, including mature cDC, into the TME.

The in vivo administration of ED31 as a monotherapy could neither induce immune cell infiltration nor exert an antitumor effect; ED31 must be combined with anti-CTLA-4, not with anti-PD-1, to show antitumor efficacy. ED31 as a single agent promoted chemokine-producing capacity of BM-Mϕ in vitro, but not in vivo Mϕ in the TME. Therefore, one possible reason could be that Mϕ in the TME are under dual immunosuppressive signals that need to be released simultaneously through the combination therapy of ED31 and anti-CTLA-4. It is unlikely that anti-CTLA-4 directly acts on Mϕ since CTLA-4 is expressed exclusively on T cells, not on the Mϕ per se.[40] Indeed, we confirmed that BM-Mϕ have no expression of CTLA-4, and in vitro anti-CTLA-4 exposure of BM-Mϕ had no effect on the chemokine-producing capacity nor on surface marker expression (online supplemental figures 4 and 5). Anti-CTLA-4 is known to block the interaction of CTLA-4 on T-cell populations with CD80 and CD86 on DC and thus strongly enhances T-cell immunity.[41] Thus, the increase of $CD86^{+}$ mature cDC in the TME, only detected in the combination of ED31 with anti-CTLA-4, might be the important change in eliciting superior antitumor efficacy compared with the monotherapies. The presence of mature cDC in the TME has been shown to be associated with favorable prognosis in a variety of cancer types.[42 43] Moreover, mature cDC is the essential composition of tertiary lymphoid structures (TLS), which are associated with improved clinical outcomes and responses to certain cancer immunotherapies. TLS might be one of the destinations for infiltrating mature cDC.[44–48] Taken together with our findings that neither ED31 monotherapy nor anti-CTLA-4 monotherapy could increase the density of mature cDC in the TME (figure 2E) and the combination therapy against cDC_1 knockout mice failed to increase the variety of immune cell infiltrates in the TME (figure 5F–H), one of the possible reasons why ED31 was needed to be administered with anti-CTLA-4 was that cDC and Mϕ affect each other closely in the TME, and this novel combination therapy promotes maturation of cDC and simultaneously releases another suppressive signal against Mϕ that conferred the increase of chemokine production and effective immune cell infiltration with mature cDC in the TME. We also demonstrated several immune effector cells contributing to the therapeutic effect elicited by the combination of ED31 and anti-CTLA-4, including NK cells. Some studies showed that B16 melanoma may require NK cells for tumor growth control[18] and intratumoral NK cells can

contribute to the recruitment of cDC into the TME.[39 42] This combination therapy could not only induce rapid immune cell infiltration into the TME, but also might enhance T-cell clonal expansion over time by harnessing cDC-T cell cross talk within the TME. Notably, the early initiation of this combination therapy showed durable complete responses in almost all the mice (figure 1A–C). In addition to the fact that this combination can induce superior tumor-antigen specific CTL infiltration in the TME (online supplemental figure 2), it is speculated that using this therapy in neoadjuvant/adjuvant settings may also be one of the promising approaches for high-risk patients to reduce the recurrence risk by harnessing the cDC-T cell priming phase without the use of specific tumor antigens.

A previous study using ED31 demonstrated that targeting MARCO by ED31 can result in high major histocompatibility complex class II expression on Mϕ within the TME.[16] In our study, we demonstrated Mϕ reprogramming by focusing on chemokine production. Our analysis revealed that ED31 could induce chemokine production by Mϕ in an M1 pattern. We had attempted to show this reprogramming by surface marker expression changes on Mϕ.[9] However, we were unable to detect changes in several surface markers on Mϕ following in vitro ED31 exposure (online supplemental figure 5). Thus, we applied chemokine analysis to elucidate the mechanism of the significant increase of immune cell infiltration into the TME. While Mϕ plasticity is well-established,[11 49] we suggest that functional analysis focusing on chemokine production rather than on an analysis of surface markers may be more direct to discriminate various functional phenotypes of Mϕ in the TME.

In recent years, therapeutic approaches targeting scavenger receptors have begun to attract attention.[50] Scavenger receptors including MARCO were identified by their ability to recognize and remove substances that are harmful to the body, such as oxidized fatty acids and various pathogens.[8 11–13] In tumor tissues, various debris derived from cancer cells could bind to these receptors as ligands, and, as a result, cause undesirable effects within the TME. In our study, it is possible that dead tumor cell ligand-binding to MARCO on Mϕ in the TME could inhibit chemokine production by the Mϕ, resulting in suppression of immune cell infiltration. Therefore, this ligand-binding on MARCO in the TME could serve as one of the potential mechanisms to explain the paucity of immune cell infiltration, and inhibition of ligand-binding on MARCO by ED31 overcoming the suppressed function of Mϕ. Notwithstanding, since Mϕ have a variety of functions in addition to chemokine production, there remains a further need to elucidate the tangled mechanisms beyond the chemokines induced by targeting MARCO in combination with anti-CTLA-4. Moreover, the immunologic crosstalk between the TME and TLS, with particular attention to cDC migration, needs to be investigated as well. The future direction of our research should also include whether adding anti-PD-1/PD-L1 sequentially after this combination therapy of anti-CTLA-4 and ED31 may enhance the antitumor efficacy further.

In conclusion, we have revealed the significance of targeting MARCO in combination with anti-CTLA-4. This unique combination can reprogram and use Mϕ in the TME to induce an M1-pattern of chemokine production, resulting in a notable increase of various immune cell types, together with mature cDC, that infiltrate the TME and activation through anti-CTLA-4. We believe our studies reported here serve as strong rationale for the clinical application of targeting MARCO in combination with anti-CTLA-4 in patients with cancer, particularly in cases of ICI failures.

X Rana Falahat @RanaFalahat

Acknowledgements This work has been supported by the Moffitt/USF Vivarium, Flow Cytometry Core, Tissue Histology Core, and Analytic Microscopy Core; all comprehensive cancer center facilities designated by the National Cancer Institute (P30-CA076292). HT would like to thank Drs Etsuko Aruga and Atsushi Aruga for their support behind this work. Some of the results in this study were presented at the American Association for Cancer Research Annual Meeting 2024 (San Diego, California, USA, Cancer Res 2024;84(6_Suppl):3918).

Contributors All authors designed research. HT and PP-V performed research. HT and PP-V analyzed data. HT and JJM wrote the paper. All authors reviewed and edited the paper. JJM is the guarantor.

Funding This work was funded by the NCI-NIH (1R01 CA148995, 1R01 CA184845, P30 CA076292, P50 CA168536), CJG Fund, Chris Sullivan Fund, V Foundation, and the Dr. Miriam and Sheldon G. Adelson Medical Research Foundation (to JJM).

Competing interests JJM has ownership interest in Aleta Biotherapeutics, CG Oncology, Turnstone Biologics, Ankyra Therapeutics, and AffyImmune Therapeutics, and is a paid consultant/paid scientific and/or clinical advisory board member for Turnstone Biologics, Vault Pharma, Ankyra Therapeutics, AffyImmune Therapeutics, UbiVac, Vycellix, and Aleta Biotherapeutics, as well as a Board of Directors member of CG Oncology.

Patient consent for publication Not applicable.

Ethics approval Not applicable.

Provenance and peer review Not commissioned; externally peer reviewed.

Data availability statement Data are available upon reasonable request. All data relevant to the study are included in the article or uploaded as supplementary information.

ORCID iDs
Hidenori Takahashi http://orcid.org/0000-0001-7872-1519
Patricio Perez-Villarroel http://orcid.org/0000-0003-1997-5994
Rana Falahat http://orcid.org/0000-0001-7489-3807
James J Mulé http://orcid.org/0000-0001-7354-0516

REFERENCES

1 Hodi FS, O'Day SJ, McDermott DF, *et al*. Improved survival with ipilimumab in patients with metastatic melanoma. *N Engl J Med* 2010;363:711–23.
2 Postow MA, Chesney J, Pavlick AC, *et al*. Nivolumab and ipilimumab versus ipilimumab in untreated melanoma. *N Engl J Med* 2015;372:2006–17.
3 Ribas A, Wolchok JD. Cancer immunotherapy using checkpoint blockade. *Science* 2018;359:1350–5.
4 Wolchok JD, Chiarion-Sileni V, Gonzalez R, *et al*. Long-Term Outcomes With Nivolumab Plus Ipilimumab or Nivolumab Alone Versus Ipilimumab in Patients With Advanced Melanoma. *J Clin Oncol* 2022;40:127–37.
5 Mellman I, Chen DS, Powles T, *et al*. The cancer-immunity cycle: Indication, genotype, and immunotype. *Immunity* 2023;56:2188–205.
6 Zhu Y, Knolhoff BL, Meyer MA, *et al*. CSF1/CSF1R blockade reprograms tumor-infiltrating macrophages and improves response to T-cell checkpoint immunotherapy in pancreatic cancer models. *Cancer Res* 2014;74:5057–69.
7 Cassetta L, Pollard JW. A timeline of tumour-associated macrophage biology. *Nat Rev Cancer* 2023;23:238–57.
8 Canton J, Neculai D, Grinstein S. Scavenger receptors in homeostasis and immunity. *Nat Rev Immunol* 2013;13:621–34.
9 DeNardo DG, Ruffell B. Macrophages as regulators of tumour immunity and immunotherapy. *Nat Rev Immunol* 2019;19:369–82.
10 Mok S, Koya RC, Tsui C, *et al*. Inhibition of CSF-1 receptor improves the antitumor efficacy of adoptive cell transfer immunotherapy. *Cancer Res* 2014;74:153–61.
11 Mantovani A, Allavena P, Marchesi F, *et al*. Macrophages as tools and targets in cancer therapy. *Nat Rev Drug Discov* 2022;21:799–820.
12 Elomaa O, Kangas M, Sahlberg C, *et al*. Cloning of a novel bacteria-binding receptor structurally related to scavenger receptors and expressed in a subset of macrophages. *Cell* 1995;80:603–9.
13 van der Laan LJ, Döpp EA, Haworth R, *et al*. Regulation and functional involvement of macrophage scavenger receptor MARCO in clearance of bacteria in vivo. *J Immunol* 1999;162:939–47.
14 Brunner JS, Vogel A, Lercher A, *et al*. The PI3K pathway preserves metabolic health through MARCO-dependent lipid uptake by adipose tissue macrophages. *Nat Metab* 2020;2:1427–42.
15 Bergamaschi A, Tagliabue E, Sørlie T, *et al*. Extracellular matrix signature identifies breast cancer subgroups with different clinical outcome. *J Pathol* 2008;214:357–67.
16 Georgoudaki A-M, Prokopec KE, Boura VF, *et al*. Reprogramming Tumor-Associated Macrophages by Antibody Targeting Inhibits Cancer Progression and Metastasis. *Cell Rep* 2016;15:2000–11.
17 La Fleur L, Boura VF, Alexeyenko A, *et al*. Expression of scavenger receptor MARCO defines a targetable tumor-associated macrophage subset in non-small cell lung cancer. *Int J Cancer* 2018;143:1741–52.
18 Eisinger S, Sarhan D, Boura VF, *et al*. Targeting a scavenger receptor on tumor-associated macrophages activates tumor cell killing by natural killer cells. *Proc Natl Acad Sci U S A* 2020;117:32005–16.
19 La Fleur L, Botling J, He F, *et al*. Targeting MARCO and IL37R on Immunosuppressive Macrophages in Lung Cancer Blocks Regulatory T Cells and Supports Cytotoxic Lymphocyte Function. *Cancer Res* 2021;81:956–67.
20 Jeremiasen M, Borg D, Hedner C, *et al*. Tumor-Associated CD68+, CD163+, and MARCO+ Macrophages as Prognostic Biomarkers in Patients With Treatment-Naïve Gastroesophageal Adenocarcinoma. *Front Oncol* 2020;10:534761.
21 Chen AX, Gartrell RD, Zhao J, *et al*. Single-cell characterization of macrophages in glioblastoma reveals MARCO as a mesenchymal pro-tumor marker. *Genome Med* 2021;13:88.
22 Shi B, Chu J, Huang T, *et al*. The Scavenger Receptor MARCO Expressed by Tumor-Associated Macrophages Are Highly Associated With Poor Pancreatic Cancer Prognosis. *Front Oncol* 2021;11:771488.
23 Grolleau A, Misek DE, Kuick R, *et al*. Inducible expression of macrophage receptor Marco by dendritic cells following phagocytic uptake of dead cells uncovered by oligonucleotide arrays. *J Immunol* 2003;171:2879–88.
24 Matsushita N, Komine H, Grolleau-Julius A, *et al*. Targeting MARCO can lead to enhanced dendritic cell motility and anti-melanoma activity. *Cancer Immunol Immunother* 2010;59:875–84.
25 Komine H, Kuhn L, Matsushita N, *et al*. Examination of MARCO activity on dendritic cell phenotype and function using a gene knockout mouse. *PLoS One* 2013;8:e67795.
26 Banchereau J, Steinman RM. Dendritic cells and the control of immunity. *Nature New Biol* 1998;392:245–52.
27 Moynihan KD, Opel CF, Szeto GL, *et al*. Eradication of large established tumors in mice by combination immunotherapy that engages innate and adaptive immune responses. *Nat Med* 2016;22:1402–10.
28 Phan GQ, Attia P, Steinberg SM, *et al*. Factors associated with response to high-dose interleukin-2 in patients with metastatic melanoma. *J Clin Oncol* 2001;19:3477–82.
29 Nagarsheth N, Wicha MS, Zou W. Chemokines in the cancer microenvironment and their relevance in cancer immunotherapy. *Nat Rev Immunol* 2017;17:559–72.
30 Mempel TR, Lill JK, Altenburger LM. How chemokines organize the tumour microenvironment. *Nat Rev Cancer* 2024;24:28–50.
31 Galon J, Bruni D. Approaches to treat immune hot, altered and cold tumours with combination immunotherapies. *Nat Rev Drug Discov* 2019;18:197–218.
32 Yagawa Y, Robertson-Tessi M, Zhou SL, *et al*. Systematic Screening of Chemokines to Identify Candidates to Model and Create Ectopic Lymph Node Structures for Cancer Immunotherapy. *Sci Rep* 2017;7:15996.
33 Coppola D, Nebozhyn M, Khalil F, *et al*. Unique ectopic lymph node-like structures present in human primary colorectal carcinoma are identified by immune gene array profiling. *Am J Pathol* 2011;179:37–45.
34 Messina JL, Fenstermacher DA, Eschrich S, *et al*. 12-Chemokine gene signature identifies lymph node-like structures in melanoma: potential for patient selection for immunotherapy? *Sci Rep* 2012;2:765.
35 Prabhakaran S, Rizk VT, Ma Z, *et al*. Evaluation of invasive breast cancer samples using a 12-chemokine gene expression score: correlation with clinical outcomes. *Breast Cancer Res* 2017;19:71.
36 Harlin H, Meng Y, Peterson AC, *et al*. Chemokine expression in melanoma metastases associated with CD8+ T-cell recruitment. *Cancer Res* 2009;69:3077–85.
37 Kohli K, Pillarisetty VG, Kim TS. Key chemokines direct migration of immune cells in solid tumors. *Cancer Gene Ther* 2022;29:10–21.
38 Spranger S, Bao R, Gajewski TF. Melanoma-intrinsic β-catenin signalling prevents anti-tumour immunity. *Nature New Biol* 2015;523:231–5.
39 Böttcher JP, Bonavita E, Chakravarty P, *et al*. NK Cells Stimulate Recruitment of cDC1 into the Tumor Microenvironment Promoting Cancer Immune Control. *Cell* 2018;172:1022–37.
40 Pardoll DM. The blockade of immune checkpoints in cancer immunotherapy. *Nat Rev Cancer* 2012;12:252–64.
41 Qureshi OS, Zheng Y, Nakamura K, *et al*. Trans-endocytosis of CD80 and CD86: a molecular basis for the cell-extrinsic function of CTLA-4. *Science* 2011;332:600–3.
42 Barry KC, Hsu J, Broz ML, *et al*. A natural killer-dendritic cell axis defines checkpoint therapy-responsive tumor microenvironments. *Nat Med* 2018;24:1178–91.
43 Del Prete A, Salvi V, Soriani A, *et al*. Dendritic cell subsets in cancer immunity and tumor antigen sensing. *Cell Mol Immunol* 2023;20:432–47.
44 Cabrita R, Lauss M, Sanna A, *et al*. Tertiary lymphoid structures improve immunotherapy and survival in melanoma. *Nature New Biol* 2020;577:561–5.
45 Goc J, Germain C, Vo-Bourgais TKD, *et al*. Dendritic cells in tumor-associated tertiary lymphoid structures signal a Th1 cytotoxic immune contexture and license the positive prognostic value of infiltrating CD8+ T cells. *Cancer Res* 2014;74:705–15.
46 Sautès-Fridman C, Petitprez F, Calderaro J, *et al*. Tertiary lymphoid structures in the era of cancer immunotherapy. *Nat Rev Cancer* 2019;19:307–25.
47 Aoyama S, Nakagawa R, Mulé JJ, *et al*. Inducible Tertiary Lymphoid Structures: Promise and Challenges for Translating a New Class of Immunotherapy. *Front Immunol* 2021;12:675538.
48 Xiao Z, Wang R, Wang X, *et al*. Impaired function of dendritic cells within the tumor microenvironment. *Front Immunol* 2023;14:1213629.
49 Liu SX, Gustafson HH, Jackson DL, *et al*. Trajectory analysis quantifies transcriptional plasticity during macrophage polarization. *Sci Rep* 2020;10:12273.
50 Xu S, Chaudhary O, Rodríguez-Morales P, *et al*. Uptake of oxidized lipids by the scavenger receptor CD36 promotes lipid peroxidation and dysfunction in CD8$^+$ T cells in tumors. *Immunity* 2021;54:1561–77.